Journal of Autoimmunity 105 (2019) 102290

Contents lists available at ScienceDirect

Journal of Autoimmunity

journal homepage: www.elsevier.com/locate/jautimm

Myeloid sphingosine-1-phosphate receptor 1 is important for CNS autoimmunity and neuroinflammation☆

Hsing-Chuan Tsai[a], Khoa Nguyen[b], Ezzat Hashemi[a], Edgar Engleman[b], Timothy Hla[c], May H. Han[a,*]

[a] Department of Neurology and Neurological Sciences, Stanford University, Stanford, CA, USA
[b] Department of Pathology, Stanford University School of Medicine (Blood Center), Palo Alto, CA, USA
[c] Vascular Biology Program, Boston Children's Hospital, Department of Surgery, Harvard Medical School, Boston, MA, USA

ARTICLE INFO

Keywords:
Multiple sclerosis
Sphingosine-1-phosphate receptor 1
Signal transducer and activator of transcription 3 (STAT3)
Interleukin 6
Myeloid cells

ABSTRACT

The critical role of sphingosine-1-phosphate (S1P) signaling in lymphocyte trafficking is well recognized, however, the contribution of myeloid cell-S1P signaling in neuroimmunity is less well understood. We previously reported that C57BL/6J mice harboring phosphorylation defective S1P receptor 1 ($S1P_1$) (with mutated serines in the carboxyl terminus, leading to impaired receptor internalization) [$S1P_1$(S5A)] developed severe, T_H17-dominant experimental autoimmune encephalomyelitis. In this study, we demonstrate that $S1P_1$-mediated T_H17 polarization is not an intrinsic T cell effect, but dependent on sustained $S1P_1$ signaling in myeloid cells. First, utilizing the $S1P_1$(S5A) mice in the EAE model, we observed that $S1P_1$ activated and enhanced antigen presentation function in myeloid cells. Second, sequential phosphorylation of STAT3 occurred in dendritic cells, monocytes, and macrophages/microglia during neuroinflammation. Third, we show that pro-inflammatory ($CD45^{hi}CD11b^{+}Ly6C^{hi}$) monocytes contribute to T_H17 differentiation and neuroinflammation by regulating IL-6 expression. Finally, results from experiments utilizing myeloid cell-specific $S1P_1$ overexpression (*S1pr1*$^{f/stop/f}$:*LysM*^{Cre}) mice demonstrate that myeloid cell $S1P_1$ directly contributes to severity of neuroinflammation. These findings reveal the critical contribution of myeloid-$S1P_1$ signaling in CNS autoimmunity.

1. Introduction

Functionally distinct myeloid cells contribute to the initiation, establishment and outcome of central nervous system (CNS) autoimmunity by exerting their antigen presentation function, modulating neuroinflammation and removal of myelin debris [1–4]. Persistent macrophage and microglia activation is observed in the CNS of MS patients, for months to years, and is considered a significant contributor of secondary progressive MS [5]. Therapies for MS, including glatiramer acetate, dimethyl fumarate and cholecalciferol (vitamin D3), regulate myeloid cell function [4]; however, direct myeloid cell-targeted therapies are lacking.

Sphingosine-1-phosphate (S1P) and its receptors ($S1P_{1-5}$) signaling is a major targetable pathway in MS therapeutics [6]. FTY720 (Gilenya®) and BAF312 (Siponimod), a first line and a Phase III investigational study for treatment of MS, target $S1P_1$ in lymphocytes, and retain them within the secondary lymphoid organs [7–11]. Mechanistically, binding of S1P to $S1P_1$ initiates β-arrestin recruitment, C-terminal serine phosphorylation by protein kinase GRK2, followed by downstream signaling. The signal is terminated by the internalization of S1P-S1PR complex [12]. Failure to internalize $S1P_1$ in lymphocytes results in prolonged surface residence of $S1P_1$ and impaired response to retain lymphocytes in response to FTY-720 treatment [13,14]. However, the effects of $S1P_1$ surface residence in other immune cells are not known.

Our previous work has demonstrated that a genetically modified mouse model, $S1P_1$(S5A) mice, carrying phosphorylation defective *S1pr1* (resulting in impaired internalization of $S1P_1$) developed severe T_H17-mediated autoimmune CNS demyelination by activating the IL-6/JAK/STAT3 pathway in the myelin oligodendrocyte glycoprotein $(MOG)_{35\text{-}55}$-immunized experimental autoimmune encephalomyelitis (EAE) model [15]. We further extended our study to investigate how

---

Abbreviations: EAE, Experimental autoimmune encephalomyelitis; MOG, myelin oligodendrocyte glycoprotein; $S1P_1$, sphingosine-1-phosphate receptor 1; DCs, dendritic cells

☆ The authors have declared that no conflict of interest exists.

* Corresponding author. 1201 Welch Road, MSLS, P212 Stanford, CA, 94305, USA.
E-mail address: mayhan@stanford.edu (M.H. Han).

https://doi.org/10.1016/j.jaut.2019.06.001
Received 3 April 2019; Received in revised form 28 May 2019; Accepted 1 June 2019

S1P signaling in myeloid cells contribute to T_H17 autoimmunity and neuroinflammation. In the current study, utilizing the $S1P_1$(S5A) EAE model, we observed that the surface residence of $S1P_1$ enhanced activation of dendritic cells (DCs), monocytes and microglia. We also observed that proinflammatory monocytes provide IL-6, an essential cytokine for T_H17 differentiation. In addition, we show that $S1P_1$-STAT3 activation in different immune compartments during initiation, establishment and progression of EAE. Finally, experiments with myeloid cell overexpression and knockout mice demonstrate that $S1P_1$ signaling in different myeloid cell subsets contribute to neuroinflammation in multiple mechanisms.

2. Materials and methods

2.1. Mice

$S1P_1$(S5A) mice on C57BL/6J background were generated as previously described [13]. *S1pr1*$^{f/f}$ mice were provided by Dr. Richard Proia (NIDDK, NIH) [16]. *S1pr1*$^{f/f}$ mice were crossed with *Rosa26-Cre-ER*^{T2} mice (Jackson Laboratory) to generate *S1pr1*$^{f/f}$ *Rosa26*$^{Cre-ERT2}$ ($S1P_1$ KO mice) or with *Lysm-Cre* mice for *S1pr1*$^{f/f}$*:LysM*^{Cre} ($S1P_1$ LysM KO mice). *S1pr1*$^{fstop//f}$ mice [17] were crossed with LysM-Cre (Jackson Laboratory) to generate *S1pr1*$^{f/stop/f}$*:LysM*^{Cre} ($S1P_1$ LysM OE mice). The C57BL/6J MOG_{35-55}–specific TCR-Tg (2D2, TCR^{MOG}) mice were from Jackson Laboratory. Mice were housed in 12-hr light/dark cycle and were given food and water ad libitum. Animal experiments were approved by the Institutional Animal Care and Use Committee at Stanford University and performed in compliance with the US National Institutes of Health guidelines provided by the committee.

2.2. Reagents

FTY720 (S)-Phosphate (FTY720p; CAS 402616-26-6) was purchased from Cayman Chemical. Anti-CD3 (clone 145-2C11) and anti-CD28 (clone 37.51) antibodies were purchased from Biolegend. Mouse recombinant IL-6 (406-ML), IL-12 (419-ML), IL-23 (1887-ML), and TGF-β (7666-MB) were purchased from R&D Systems and Liberase enzyme cocktail was from Roche Biosciences. Monoclonal antibodies for flow cytometry analysis were purchased from the following sources; anti-CD45 (clone 30-F11), anti-CD3 (clone 145-2c11), anti-CD8 (clone 53–6.7), and anti-IFN-γ (clone XMG-1.2) were from BD Biosciences; anti-CD11b (clone M1/70), anti-CD11c (clone N418), abti-Ly6C (clone HK1.4), anti-Ly6G (clone 1A8), anti-IL-6 (clone MP5-20F3), anti-STAT3 phospho Tyr705 (clone 13A3-1) and anti-CD4 (clone GK1.5) were from Biolegend, and anti-IL-17 (clone ebio17B7) was from eBioscience. The anti-CD40L neutralizing antibody (clone 208109) was purchased from R&D Systems.

2.3. EAE experiments

$S1P_1$(S5A) mice and wild-type (WT) C57BL/6J mice were housed in the Research Animal Facility at Stanford University. EAE was induced in 8-12-week-old female WT, $S1P_1$(S5A), $S1P_1$ LysM OE, and $S1P_1$ LysM KO mice immunized with an emulsion containing 200 μg Complete Freund's Adjuvant (CFA), 100 μg myelin oligodendrocyte glycoprotein (MOG) peptide$_{35–55,}$ and 200 ng *Bordetella pertussis* toxin (lot# 181236A1, List Biological Laboratories) on days 0 and 2. Typical EAE clinical symptoms were scored as follows: 0, normal; 1, tail paralysis; 2, hind limb weakness; 3, complete hind limb paralysis; 4, hind limb paralysis with forelimb weakness; and 5, moribund or death [18]. Atypical EAE symptoms observed in the $S1P_1$ LysM OE mice were scored, separately from EAE, as follows: 0, normal; 1, hunched posture and head tilt; 2, head tilt, mild ataxia and/or kyphosis; 3, pronounced ataxia and/or kyphosis; 4, severe proprioception impairment; 5, moribund. This scoring criteria was modified from Stromnes IM [19].

2.4. Characterization of CNS immune cells

Immune cells from the CNS tissue were isolated based on the methods outlined in Arac et al. [20]. Immune cells were labeled with monoclonal antibodies against CD45, CD3, CD4, CD8, CD11b, CD11c, Ly6C, Ly6G, I-A/E, CD40 and CD86. For intracellular staining of IL-6, immune cells were activated *in vitro* with 500 ng/ml LPS in the presence of Golgi-plug (BD Biosciences) for 6 h. Cells were then labeled with anti–IL-6 antibodies. For intracellular staining of IL-17A, immune cells were activated with 50 ng/ml phorbol 12-myristate, 13-acetate (PMA) and 500 ng/ml ionomycin for 4-6 h and then labeled with anti-IL17A antibodies. $0.5–1 \times 10^6$ cells labeled with respective antibodies were analyzed by a LSRII Flow Cytometer (BD) at the Stanford Shared Flow Facility. BD FACSDiva 6.0 software was used to acquire data and FlowJo was used for data analysis (Tree Star).

2.5. In vitro T_H17 polarization

$CD4^+$ T cells were isolated from spleens of 8-12-week-old naïve WT and $S1P_1$(S5A) mice utilizing magnetic CD4 microbeads (Miltenyi Biotec). Cells were then cultured in RPMI 1640 media supplemented with 10% FBS for 5 days in 24-well plates pre-coated with anti-mouse CD3 (5 μg/ml) and CD28 (2 μg/ml) under T_H17 polarization condition [IL-6 (20 ng/ml), IL-23 (20 ng/ml), TGF-β (1 ng/ml), anti-IFN-γ (5 μg/ml), and anti-IL-4 (5 μg/ml) antibodies] in the presence of S1P (250 nM), AUY950 (10 nM), W146 (1 μM), FTY720p (250nM-1μM) or vehicle (DMSO) as indicated. Cells were harvested on day 5, activated with 50 ng/ml PMA and 500 ng/ml ionomycin in the presence of Golgi-plug (BD Biosciences) for 4 h, labeled with anti- IFN-γ, IL-17A and analyzed by LSRII Flow cytometry (BD) for intracellular cytokine staining as previously described [14].

2.6. Antigen presenting cells and T cell co-culture experiment

$CD4^+$ T cells (CD4 MicroBeads kit, Miltenyi Biotec) isolated from 2D2 T cell receptor transgenic (TCR^{MOG}) mice [21] were co-cultured with either 1) CD4-depleted, irradiated (30Gy) splenocytes or 2) purified irradiated splenic $CD11b^+$ cells (CD11b MicroBeads kit, Miltenyi Biotec) from pre-symptomatic (day 7) MOG_{35-55}-immunized WT or $S1P_1$(S5A) EAE mice in RPMI medium supplemented with 10% FBS in round-bottom culture plates at indicated ratios (1:1, 1:5, 1:10). Cells were reactivated with MOG_{35-55} (0-20 μg/ml) for 2-4 days and culture supernatant was analyzed for IL-17A, IFNγ and IL-6 expression by ELISA according to the manufactuer's instructions (R&D systems and BD Biosciences). Cell proliferation was also measured by alamarBlue Cell Viability Assay (Invitrogen) from 72 to 96 h.

2.7. Bonemarrow-derived dendritic cell/Macrophage cultures

Bone marrow cells isolated from mouse femurs and tibias were cultured for 7 days in the presence of GM-CSF (25 ng/ml) and IL-4 (50 ng/ml) to differentiate into DCs or M-CSF (10 ng/ml) to differentiate into macrophages [22]. Bone marrow-derived DCs or macrophages were then activated with LPS (100–500 ng/ml) or CpG (0.5 μM) for 4-6 h with or without Golgiplug. IL-6 expression from the culture supernatant was measured by ELISA or intracellular staining of IL-6 was measured by flow cytometry.

2.8. Immunoblot analysis

Protein extracts was prepared in Radioimmunoprecipitation assay (RIPA) buffer supplemented with Halt protease inhibitor and phosphatase inhibitors (Roche Applied Sciences). The protein homogenate was quantified by the BCA assay (Thermo Scientific), and 50-100ug of the sample was resolved on 4–12% Bis–Tris SDS–PAGE gels (Life Technologies), transferred to PVDF membrane, blocked with 3% BSA in

TBST buffer at room temperature for 1 h, and labeled with primary anti-STAT3 phospho Tyr705 (D3A7, Cell Signaling) and p65 phospho Ser536 antibodies (93H1, Cell Signaling) overnight, followed by hybridization with species-specific fluorochrome-conjugated secondary antibody. The anti-β-actin antibody (4C2, Sigma-Aldrich) was used as control.

2.9. *Statistical analyses*

Data represent the mean ± SEM. Mann-Whitney *U*-test was performed for comparison of EAE clinical scores. One-way ANOVA and Tukey's multiple comparison test was used to determine significance between 3 or more test groups. Two-tailed Student's *t*-test was used for direct comparison of 2 groups. A *p* value of less than 0.05 was considered statistically significant.

3. Results

3.1. *$S1P_1$ signaling mediates pronounced myeloid cell activation*

We have previously shown that mice carrying phosphorylation deficient $S1P_1$ [$S1P_1$(S5A) mice] developed early onset and more severe T_H17-dominant neuroinflammation [15]. Here, we extend our studies to investigate how myeloid cell-$S1P_1$ signaling contributes to T_H17 differentiation and autoimmune neuroinflammation. We performed flow cytometry to characterize myeloid cell subsets and their functional status in the spleen and CNS of $S1P_1$(S5A) and WT (C57BL/6J) mice during the EAE disease course [naïve (day 0), early immunization (EAE clinical score 0, day 4), onset (EAE clinical score 0-1, day 7–8), peak disease (EAE clinical score 3-4, day 14–15)] following immunization with $MOG_{35\text{-}55}$ peptide (Fig. 1A) The gating scheme of immune profiling by flow cytometry was depicted in Supplementary Fig. 1. We observed that the splenocytes of naïve $S1P_1$(S5A) mice already have higher number of memory T cells ($CD4^+CD44^+CD62L^-$), dendritic cells (DC) ($CD11b^+CD11c^+$), and activated non-DC myeloid cells ($CD11b^+CD11c^-MHCII^+$) (Fig. 1B–G), suggesting that the surface residence of $S1P_1$ causes sustained immune activation, even prior to immunization. Similarly, prominent DC, T cells (Supplementary Figs. 2A–E) and activated monocyte signatures (Supplementary Fig. 2D-M) were also observed in the $S1P_1$(S5A) splenocytes during early immunization stage (day 4). However, at the time of EAE disease onset (day 7–8), the myeloid cell signature has normalized in the spleen (Supplementary Fig. 3), and a higher number of activated, monocytes ($CD45^{hi}CD11b^+Ly6C^+Ly6G^-CD40^{hi}I\text{-}A/E^+$) were present in the CNS of $S1P_1$(S5A) EAE mice, compared to their WT counterparts (Fig. 1K-L and Supplementary Fig. 4D). IL-6-producing activated monocytes were also increased in the CNS of $S1P_1$(S5A) EAE mice (Fig. 1M-N). The number of microglia ($CD45^{lo}CD11b^+$) remained unchanged at the onset of EAE (Fig. 1J). At the peak of EAE (day 14 post-immunization) the inflammatory myeloid cell signature was diminished (Supplementary Fig. 5), followed by T_H17 cell responses as previously reported [15]. Collectively, our results demonstrate sustained activation of $S1P_1$ on myeloid cells promotes sequential activation of DCs, proinflammatory monocytes, and T cells during EAE pathogenesis.

3.2. *$S1P_1$ promotes sequential STAT3 activation in dendritic cells, monocytes and microglia during EAE*

Our previous work and work by others have shown the connection between S1P signaling and STAT3 pathway [23–25]. We investigated whether STAT3 signaling contributes to the $S1P_1$-mediated myeloid cell activation in EAE disease initiation and progression. We performed

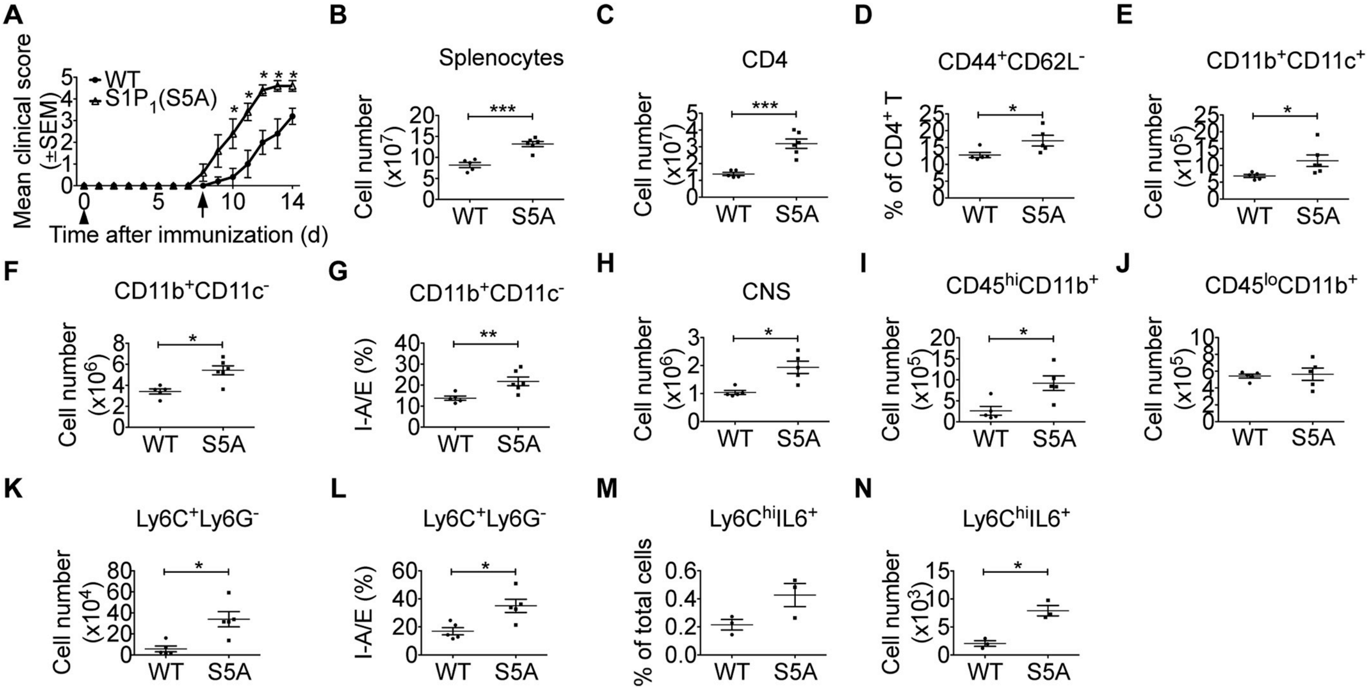

Fig. 1. Enhanced activation of monocyte-derived cells in $S1P_1$(S5A) EAE mice. (**A**) EAE disease score (mean clinical score ± SEM) of $MOG_{35\text{-}55}$-immunized C57BL/6J (WT) mice and $S1P_1$(S5A) mice and time points [triangle; day 0- (naïve) and arrow; day 8-post-immuniation (early disease onset, EAE score 0-1) where CNS and splenic immune cell profiles were analyzed by flow cytometry (n = 5, $^*p < 0.05$, Mann-Whitney *U*-test). Total number of (**B**) splenocytes, (**C**) $CD4^+$ T cells, (**D**) percentage of $CD44^+CD62L^-$ memory T cells in total $CD4^+$ T cells, (**E**) number of $CD11b^+CD11c^+$ dendritic cells, (**F**) number and (**G**) I-A/E expression (%) of $CD11b^+CD11c^-$ myeloid cells from naïve WT and $S1P_1$(S5A) mice were quantified by hemocytometer and flow cytometry. Total numbers of (**H**) CNS immune cells, (**I**) $CD45^{hi}$ myeloid cell subsets ($CD45^{hi}CD11b^+$) and (**J**) microglia ($CD45^{lo}CD11b^+$), (**K**) number and (**L**) I-A/E expression (%) of $Ly6C^+$ monocytes ($CD11b^+Ly6C^+Ly6G^-$), (**M**) percentage and (**N**) number of IL-6-expressing $Ly6C^{hi}$ monocytes from the CNS of WT and $S1P_1$(S5A) mice at d8 were quantified. Data represent 3 independent experiments except I-A/E expression, which was repeated twice (n ≥ 5/arm, mean ± SEM, $^*p < 0.05$; $^{**}p < 0.01$, two-tailed unpaired Student's *t*-test).

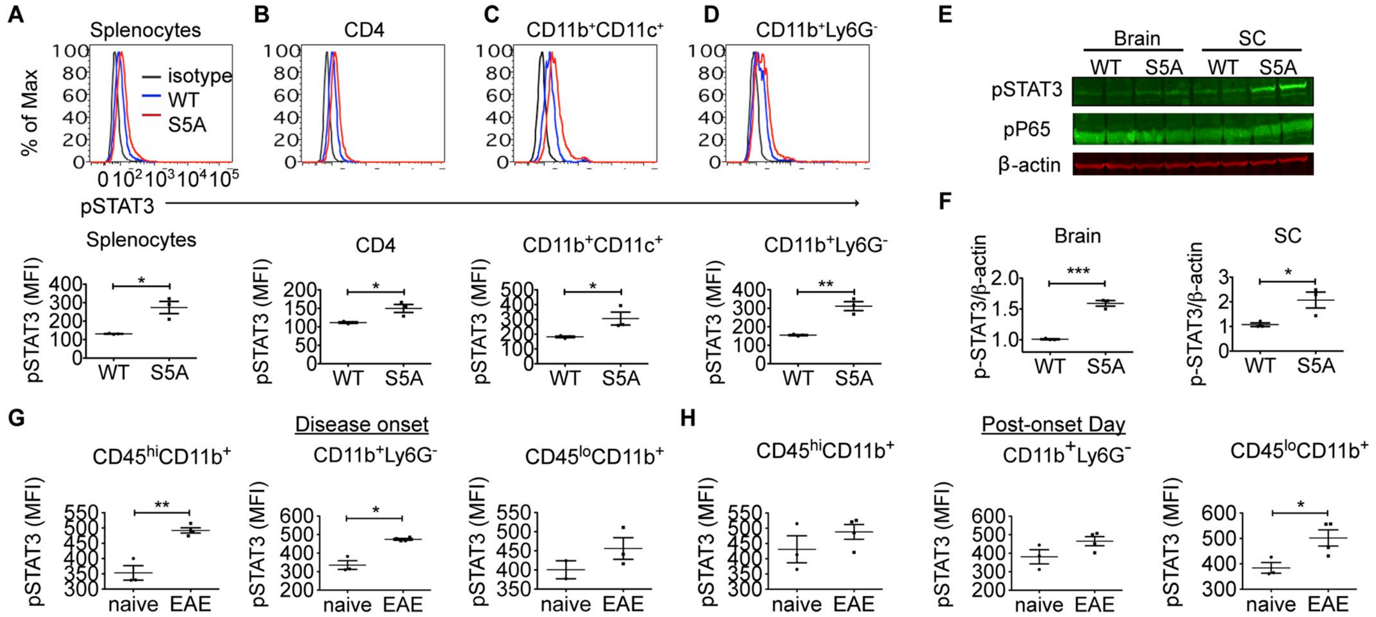

Fig. 2. S1P$_1$(S5A) myeloid cells show enhanced pSTAT3 expression. Splenocytes isolated from naïve C57BL/6J (WT) and S1P$_1$(S5A) mice were labeled with CD3, CD4, CD11b, CD11c, Ly6C, Ly6G, and pSTAT3 antibodies. The mean fluorescence intensity (MFI) of pSTAT3 in (**A**) splenocytes, (**B**) CD4$^+$ T cells, (**C**) dendritic cells (CD11b$^+$CD11c$^+$), and (**D**) mononuclear myeloid cells (CD11b$^+$Ly6G$^-$) was shown. (**E-F**) Protein extracts from the brain and spinal cord of MOG$_{35-55}$-immunized mice were analyzed by immunoblot analysis utilizing antibodies against pSTAT3, p65 and β-actin. Immune cells isolated from the CNS of naïve and EAE S1P$_1$(S5A) mice at (**G**) disease onset day or (**H**) post-onset day were labeled with CD45, CD4, CD11b, Ly6C, Ly6G, CX3CR1, and pSTAT3 antibodies. The MFI of pSTAT3 in CD45^{hi} myeloid cells (CD45^{hi}CD11b$^+$), mononuclear myeloid cells (CD11b$^+$Ly6G$^-$), and microglia (CD45^{lo}CD11b$^+$) were shown (n ≥ 3, mean ± SEM, *$p < 0.05$; **$p < 0.01$; ***$p < 0.001$, two-tailed unpaired Student's *t*-test).

phosphor-flow analysis to measure pSTAT3 expression in the splenocytes and CNS immune cells of S1P$_1$(S5A) mice during the EAE disease course. We observed enhanced pSTAT3 expression in CD4$^+$ T cells, and CD11b$^+$CD11c$^+$ DCs and CD11b$^+$Ly6G$^-$ mononuclear myeloid cells at the naïve stage (day 0) (Fig. 2A–D). During early EAE (day 4 post-immunization), splenic CD11b$^+$Ly6C$^+$Ly6G$^-$ mononuclear myeloid cells in S1P$_1$(S5A) mice showed enhanced pSTAT3 expression (Supplementary Fig. 6G). At the onset (day 7–8 post-immunization), we first observed a significant increase of STAT3 expression in the CNS tissue of S1P$_1$(S5A) mice (Fig. 2E and F and Supplementary Fig. 6I). Significant pSTAT3 activation occurred in CD45^{hi}CD11b$^+$Ly6G$^-$ mononuclear myeloid cells (Fig. 2G and Supplementary Figs. 6J–K) at the onset, followed by CNS resident microglia (CD45^{lo}CD11b$^+$) at post-onset day of EAE symptoms (day 11–12 post-immunization) (Fig. 2H) in the CNS of S1P$_1$(S5A) mice. These findings highlight the sequential, dynamic S1P$_1$-pSTAT3 signaling in the peripheral immune system during early immune activation and in the CNS during established EAE, and the contribution of myeloid cell subsets in this process.

3.3. *S1P$_1$-mediated T$_H$17 differentiation is not a T cell intrinsic effect*

We previously demonstrated that S1P$_1$(S5A) mice developed more severe EAE in the MOG$_{35-55}$-immunized and the adoptive transfer EAE models [14,15]. Existing evidence suggest that S1P$_1$ directly influences T$_H$1 and regulatory T cell balance, and modulates T$_H$17 differentiation *in vitro* [14,26,27]. Next, we explored whether S1P$_1$ –mediated T$_H$17 differentiation is a T cell intrinsic response or indirectly regulated via the antigen presenting cells. We did not observe a difference in T$_H$17 differentiation when we cultured CD4$^+$ T cells isolated from naïve S1P$_1$(S5A), WT C57BL/6J, *S1pr1*$^{f/f}$:*Rosa26*$^{\mathrm{CreERT2}}$ (S1P$_1$ KO) or control littermate mice under T$_H$17-polarizing conditions (Fig. 3A–C). Similarly, pharmacological treatment of T$_H$17 polarized cells from S1P$_1$(S5A) and WT C57BL/6J mice in culture with exogenous S1P, S1P$_1$ inhibitor (W146), or S1P$_1$ specific agonist (AUY954) also did not show significant effects on T$_H$17 differentiation (Fig. 3B and C). We also observed phosphorylated FTY720 (FTY720p) down regulated IL-17A expression only at supra-physiological concentrations (250 ng-1ug) (Fig. 3D) as previously reported [14]. Taken together, our results suggest that neither S1P$_1$ expression, surface residence, nor S1P$_1$ receptor modulation on T cells significantly altered T$_H$17 differentiation, supporting the hypothesis that S1P$_1$-mediated T$_H$17 differentiation is not a primary T cell intrinsic effect.

3.4. *S1P$_1$ signaling in the antigen presenting cells enhances T$_H$17 differentiation*

We then performed *in vitro* co-culture experiments to confirm that S1P$_1$ in myeloid cells is responsible for enhance T$_H$17 differentiation. We isolated CD4$^+$ T cells from naïve MOG$_{35-55}$-specifc, TCR transgenic 2D2 mice and co-cultured with irradiated APCs (CD4-depleted splenocytes or CD11b$^+$ myeloid cells) from MOG$_{35-55}$-immunized WT or S1P$_1$(S5A) mice (day 7 post-immunization) in the presence of MOG$_{35-55}$ peptide (0–20 μg/ml). We observed that 2D2 CD4$^+$ cells co-cultured with either S1P$_1$(S5A) CD4-depleted splenocytes or splenic CD11b$^+$ cells expressed significantly higher IL-17A expression, but not IFN-γ, compared to their WT counterparts (Fig. 4A and B). This was confirmed by T:APC co-culture with an increasing ratio of APCs (1:1, 1:5, 1:10) which also showed a linear correlation between the number of APCs in the culture with IL-17A expression (Fig. 4C) and T cell proliferation (Fig. 4D). Collectively, our data suggest that S1P$_1$ signaling in APCs is the primary driver of T$_H$17 differentiation.

3.5. *S1P$_1$-mediated IL-6 expression in myeloid cells is independent of toll-like receptor 4/9 signaling but antigen-dependent*

Our previous work suggested that S1P$_1$-mediated T$_H$17 differentiation was IL-6 dependent [15]. Since Toll-like receptor signaling (TLR) is a major pathway promoting IL-6 expression, we cultured fully differentiated bone marrow-derived dendritic cells (BMDCs) from WT and S1P$_1$(S5A) mice in the presence of LPS (100 ng/ml) and measured

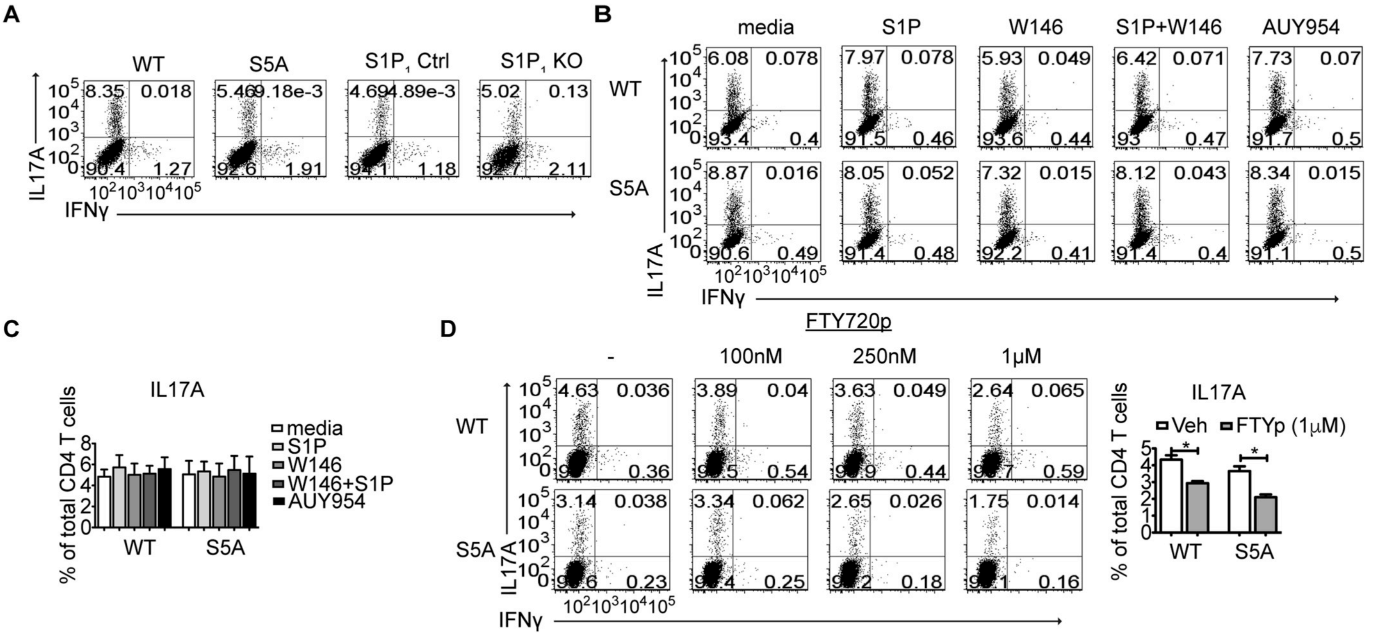

Fig. 3. $S1P_1$-mediated T_H17 differentiation is not an intrinsic T cell effect. (**A**) CD4$^+$ T cells isolated from splenocytes of naïve C57BL/6J (WT), $S1P_1$(S5A) mice *Slpr1*$^{f/f}$:*Rosa26*^{CreERT2} ($S1P_1$ *KO*) mice or their control littermates were cultured in the T_H17 differentiation medium for 5 days [anti-CD3 (5 μg/ml), anti-CD28 (2 μg/ml), IL-6 (20 ng/ml), IL-23 (20 ng/ml), and TGF-β (1 ng/ml), supplemented with 10% charcoal-treated FBS]. Cells were then restimulated with PMA (50 ng/ml) and ionomycin (500 ng/ml) for 4 h, labeled with antibodies against IFN-γ and IL-17A, and analyzed by flow cytometry. The percentage of T_H17 cells after differentiation was examined in following conditions. (**B-C**) CD4$^+$ T cells were cultured in the T_H17 differentiation medium in the presence of S1P (250 nM), W146 (1 μM), AUY954 (10 nM) added at d0, 3, and 5, and then analyzed. (**D**) CD4$^+$ T cells under T_H17-polaring condition were treated with increasing concentrations of phosphorylated FTY720 (FTYp) and analyzed by flow cytometry. Data represent 3 independent experiments (n = 3, Mean ± SEM, *$p < 0.05$, One-way ANOVA test).

intracellular and secreted IL-6 expression by intracellular cytokine staining followed by flow cytometry analysis (Fig. 5A) and ELISA of the culture supernatant (Fig. 5B) respectively. We observed that the BMDCs from $S1P_1$(S5A) mice expressed similar levels of IL-6 compared to those from WT mice. Similarly, BMDCs from $S1P_1$ KO mice did not show a significant difference compared to BMDCs from littermate controls (Fig. 5A and B). Furthermore, removal or addition of S1P, treatment with FTY720p in combination with LPS also did not have significant effects on IL-6 expression (Fig. 5C). Similar findings were also observed in experiments with bone marrow derived-macrophages or splenic CD11b and upon TLR9 agonist CpG stimulation (Supplementary Fig. 7), suggesting Toll-like receptor (TLR) 4 and 9 signaling is not a major contributor of $S1P_1$-medied IL-6 expression in APC.

Our previous work showed that splenocytes from MOG_{35-55}-immunized $S1P_1$(S5A) mice expressed high levels of IL-6 in the *ex vivo* recall assay [15]. Based on this finding, we further investigated whether $S1P_1$-mediated IL-6 expression in APCs is antigen dependent. We cultured splenocytes from MOG_{35-55}-immunized $S1P_1$(S5A) and WT mice,

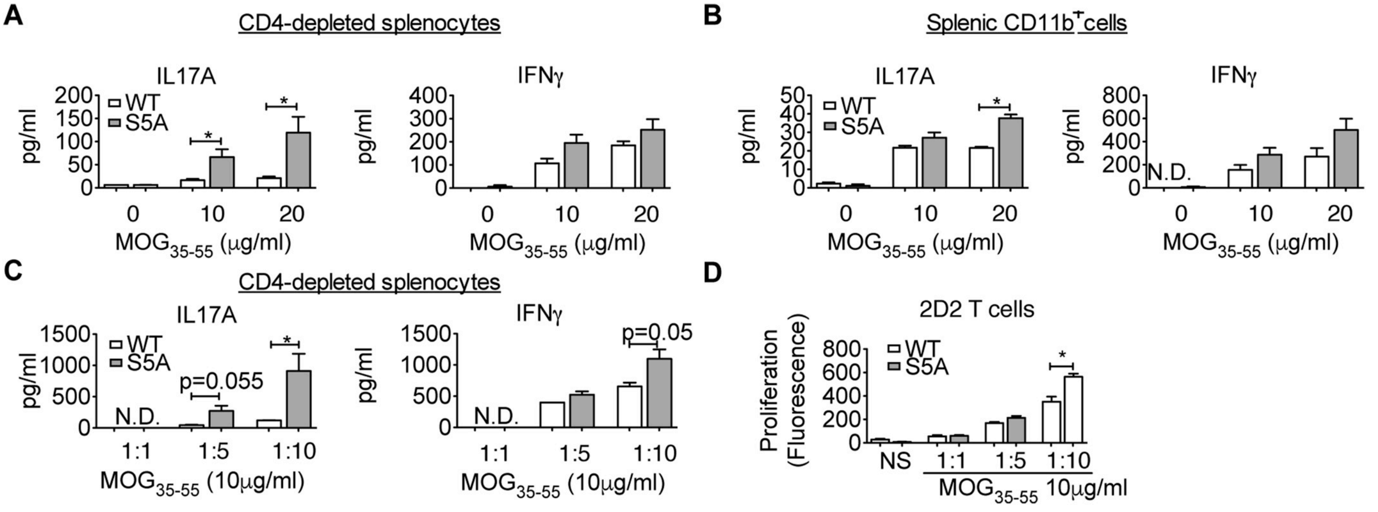

Fig. 4. Antigen-presenting cells (APCs) from $S1P_1$(S5A) mice are responsible for enhanced T_H17 differentiation. Irradiated splenocytes from MOG_{35-55}-immunized C57BL/6J (WT) and $S1P_1$(S5A) mice were further (**A**) depleted of CD4$^+$ or (**B**) selected for CD11b$^+$ cells only and then co-cultured with naïve 2D2 CD4$^+$ T cells for 48hrs in the presence of MOG_{35-55} peptide (0, 10, 20 μg/ml). Culture supernatants were examined for IL-17A and IFN-γ expression by ELISA. (**C**) CD4-depleted splenocytes were co-cultured with naïve 2D2 CD4$^+$ T cells as mentioned above in indicated T:APC ratios for 72 h and (**D**) T cell proliferation was measured by alamarBlue cell viability assay. Data represent two independent experiments (n = 3/group, each sample was analyzed in triplicates. Mean ± SEM, *$p < 0.05$; ***$p < 0.001$, two-tailed unpaired Student's *t*-test).

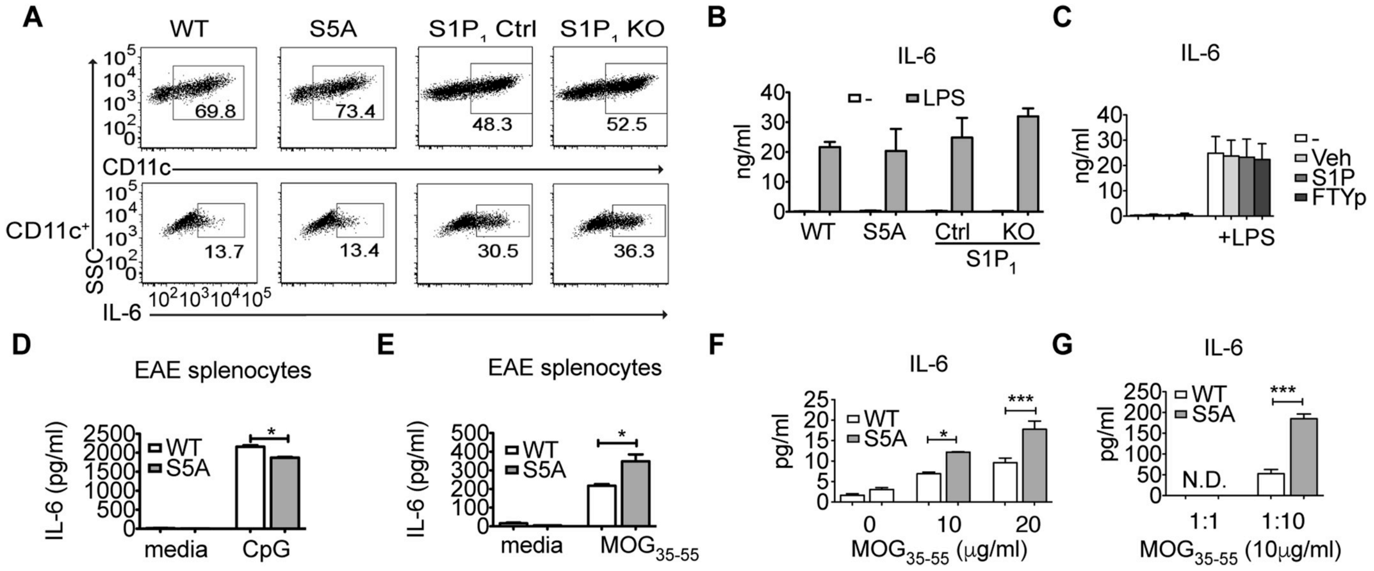

Fig. 5. S1P$_1$-enhanced IL-6 expression in myeloid cells is TLR4/9-independent and antigen-dependent. Bone marrow cells from naïve C57BL/6J (WT), S1P$_1$(S5A), S1P$_1$ KO mice and their littermates were differentiated to bone-marrow-derived dendritic cells (BMDCs) and activated by LPS for 6 h in the presence of Brefeldin A, and analyzed by (**A**) flow cytometry or the culture supernatants were examined for IL-6 expression by (**B**) ELISA (n = 3). IL-6 expression was also examined in following conditions. (**C**) BMDCs from control mice were treated with vehicle only (DMSO), S1P (250 nM), or FTY phosphates (250 nM) upon LPS stimulation. Splenocytes from MOG$_{35\text{-}55}$-immunized WT and S1P$_1$(S5A) mice were *ex-vivo* stimulated with (**D**) CpG or (**E**) MOG$_{35\text{-}55}$. 2D2 CD4$^+$ T cells were co-cultured with CD4-depleted splenocytes at (**F**) a ratio 1:5 upon MOG$_{35\text{-}55}$ stimulation in dose-dependent manner and (**G**) a high ratio of T:APC (1:10) upon MOG$_{35\text{-}55}$ stimulation (10 μg/ml) (n = 3, mean ± SEM, $*p < 0.05$; $***p < 0.001$, two-tailed unpaired Student's *t*-test). Data represent at least two independent experiments.

activated with CpG (0.5 μM) or MOG$_{35\text{-}55}$ peptides (10 μg/ml) and measured IL-6 expression in the culture supernatant by ELISA. We observed that splenocytes from S1P$_1$(S5A) mice showed less IL-6 expression to CpG treatment (Fig. 5D); however, MOG$_{35\text{-}55}$ peptides promoted high levels of IL-6 expression compared to WT mice (Fig. 5E). Furthermore, the APC: T cell co-culture assay also confirmed the dose dependent enhanced IL-6 expression with higher concentration of APCs (Fig. 5F-G).

3.6. Myeloid-specific S1P$_1$ expression influences EAE outcomes and CNS autoimmunity

We also directly tested the influence of myeloid cells S1P$_1$ signaling in CNS autoimmunity in the myeloid cell-specific S1P$_1$ over expression (*S1pr1*$^{\text{f/stop/f}}$:*LysM*$^{\text{Cre}}$, S1P$_1$ LysM OE) and S1P$_1$ deletion (*S1pr1*$^{\text{f/f}}$:*LysM*$^{\text{Cre}}$, S1P$_1$ LysM KO) in the MOG$_{35\text{-}55}$-indued EAE model. The characterization of the models and baseline immune cell profiles are depicted in Supplementary Figs. 8 and S9. We observed that the S1P$_1$ LysM OE mice developed classic EAE symptoms similar to their WT littermate controls (Fig. 6A and B and Supplementary Table 1). Interestingly, in addition, 80% of these LysM OE mice developed atypical EAE symptoms (hunched posture, head tilt, ataxia, kyphosis and impaired proprioception), absent in their littermate control counterparts (Fig. 6C and D and Supplementary Table 2). Surprisingly, the CNS S1P$_1$ LysM OE EAE mice did not show T$_{\text{H}}$17 nor pro-inflammatory monocyte signatures (Fig. 6E–G) similar to S1P$_1$(S5A) EAE mice, but indeed caused by Ly6C$^+$Ly6G$^+$ neutrophils (Fig. 6H), correlating with severity of atypical EAE symptoms (Fig. 6I). In a corollary experiment, S1P$_1$ LysM KO EAE mice showed a slight delay in onset and milder EAE symptoms compared to their littermates (Supplementary Fig. 10 and Supplementary Table 3). These results suggest that myeloid cell-S1P1 signaling indeed plays a significant role; however, can cause autoimmune neuroinflammation by multiple cellular and molecular mechanisms.

4. Discussion

In this study, we characterize for the first time the mechanisms by which myeloid cell-S1P$_1$ signaling contributes to the pathogenesis of autoimmune neuroinflammation. We demonstrate that S1P$_1$ signaling enhances antigen presentation function in monocytes by expression of MHCII and CD40. S1P$_1$ also triggers the expression of IL-6, an essential cytokine for T$_{\text{H}}$17 differentiation, in an antigen-dependent manner. In addition, S1P$_1$ signaling mitigated sequential STAT3 activation in myeloid cell subsets in the peripheral immune system and the CNS during EAE disease course. Finally, utilizing the cell-specific genetic models, we demonstrate that myeloid cell-S1P$_1$ influences the EAE clinical phenotype and outcome, highlighting the significance of myeloid cells in CNS autoimmunity.

The S1P-S1P$_1$ signal is well known for its role in lymphocyte egress. We and other groups suggest that S1P$_1$ also regulates T cell response via different mechanisms. Liu G et al. showed that S1P$_1$ directly regulates the balance of T$_{\text{H}}$1 and Treg cell via mTOR signaling [26]. Eken A et al. showed that S1P$_1$ deletion differentially affects the peripheral distribution of T$_{\text{H}}$17 and Treg cells and susceptibility to EAE by affecting their trafficking behavior [28]. Here, we suggested an alternative mechanism that S1P$_1$ regulates T$_{\text{H}}$17 response via promoting antigen-presenting functions. We discovered that APCs (DCs and pro-inflammatory monocytes) contribute to T$_{\text{H}}$17 differentiation by expressing high levels of IL-6 in an antigen-specific manner. The exact mechanism of MOG$_{35\text{-}55}$-dependent enhanced IL-6 expression remains to be deciphered. Blocking CD40L with a neutralizing antibody did not abrogate enhanced IL-6 expression from splenocytes in culture, suggesting that CD40L signaling is not a major target for this S1P$_1$-mediated IL-6 expression (Supplementary Fig. 11). Liang J et al. reported that S1P$_1$ triggers IL6 expression via a NF-κB pathway [24]. However, in our system, the p-p65 expression, a marker for NF-κB pathway, was similar between WT and S1P$_1$(S5A) mice (Fig. 2E). Ongoing experiments utilizing single cell RNA sequencing experiments will likely decipher the molecular mechanism of S1P$_1$-mediated myeloid cell activation.

Our findings also highlight the sequential and dynamic pSTAT3

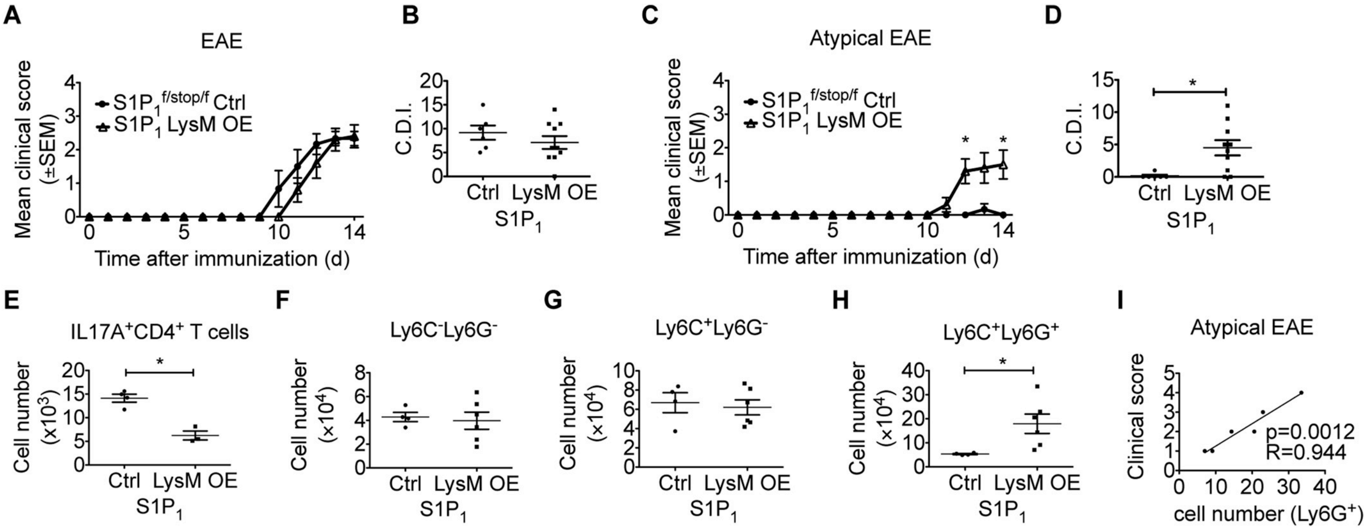

Fig. 6. Myeloid cell-$S1P_1$ over expression mice develop severe aytpical EAE. Mean clinical scores and cumulative disease index (C.D.I.) of (**A** and **B**) $^{+}$ classic EAE and (**C** and **D**) $^{++}$atypical EAE scores of MOG_{35-55} immunized *S1pr1*$^{f/sop/f}$:*LysM*^{Cre} ($S1P_1$ LysM OE) and their WT littermate controls (n ≥ 5, $*p < 0.05$, Mann-Whitney *U*-test). Data represent 2-3 independent experiments. $^{+}$ typical EAE scores (0, normal; 1, tail paralysis; 2, hind limb weakness; 3, complete hind limb paralysis; 4, hind limb paralysis with forelimb weakness; and 5, moribund or death [18]; $^{++}$atypical EAE scores (0, normal; 1, hunched posture and head tilt; 2, head tilt, mild ataxia and/or kyphosis; 3, pronounced ataxia and/or kyphosis; 4, severe proprioception impairment; 5, moribund [modified from Stromnes IM [19]]). (**E-H**) Immune cells profiles of (**E**) IL-17A-expressing $CD4^+$ T cells, (**F-G**) Mononuclear myeloid cell populations ($CD45^{hi}CD11b^+Ly6C^-Ly6G^-$), $CD45^{hi}CD11b^+Ly6C^+Ly6G^-$), and (**H**) neutrophils ($CD45^{hi}CD11b^+Ly6C^-Ly6G^+$) from the CNS of MOG_{35-55}-immunized $S1P_1$ LysM OE EAE mice (day11–12 post-immunization) were analyzed by flow cytometry (n ≥ 3, mean ± SEM, $*p < 0.05$; $***p < 0.001$, two-tailed unpaired Student's *t*-test). (**I**) The correlation of $CD45^{hi}CD11b^+Ly6C^-Ly6G^+$ neutrophils in the CNS of $S1P_1$ LysM OE EAE mice (peak disease, day 14) with severity of atypical EAE symptoms was examined by linear regression.

activation in unique immune cell subsets during EAE pathogenesis. A single-cell, multi-dimensional mass cytometry study on CNS myeloid cells of EAE mice also showed high expression on pSTAT3 in monocyte-derived myeloid cells with antigen presentation function, suggesting STAT3 signaling play a role in APC function and EAE disease progression [29]. The $S1P_1$-IL-6/STAT3 axis was also reported in tumor-associated macrophages and their contribution to tumor metastasis [23–25]. Alternatively, the $S1P_1$-mediated STAT3 activation was also observed in anti-inflammatory myeloid cell generation [30–32]. Therefore, whether $S1P_1$-STAT3 axis in myeloid cells is protective or detrimental may be context dependent.

DCs are responsible for antigen presentation and priming of adaptive immune response in the peripheral immune system. Early innate immune response in the CNS is mitigated by granulocytes and proinflammatory monocytes, whereas macrophage/microglia populations are responsible for immune surveillance and phagocytosis function [4]. In support of our findings, other groups have also reported that S1P signaling modulates the antigen presentation function of DCs and their ability to induce T_H1/T_H17 responses [33,34] and recruit myeloid cells to the inflamed tissue [35,36]. Our experiments utilizing myeloid cell $S1P_1$ over expression mice (LysM Cre OE) showed neutrophil-dominant neuroinflammation that appears to be independent of T_H17. Work by Rumble JM et al. has also shown the significant contribution of neutrophils in EAE pathogenesis [3]. Mechanistic underpinnings of $S1P_1$-mediated neutrophil activation and CNS autoimmunity remains to be explored in future experiments.

Myeloid cells are highly plastic cells and functionally distinct based on their spatial and temporal distribution during the course of autoimmune neuroinflammation [29,37–39]. A limitation in our study is how blood-derived and CNS-resident myeloid cells contribute to this process need to be further investigated. Additional experiments utilizing myeloid cell reporter mice (e.g. CX3CR1-GFP and CCR2-RFP mice), myeloid subset-specific transgenic mice, and specific markers (e.g. CD206, Arg1, iNos, Tmem119) should be included to elucidate the role of $S1P_1$ signaling in individual myeloid cell subset. The effects of S1P receptor modulators in innate immunity, including CD14 and CD16 myeloid cells, are being investigated in ongoing clinical studies [40]. The translational relevance of our findings in CNS autoimmunity and multiple sclerosis (MS) are currently ongoing in our laboratory.

In summary, these findings elucidate novel mechanisms by which myeloid cell-$S1P_1$ signaling influence the initiation and outcome of CNS autoimmunity. In the era where S1PR modulator therapies, targeting myeloid cells may also have therapeutic potentials in inflammatory and degenerative CNS disorders, including progressive MS.

Summary

$S1P_1$ signaling in myeloid cells influences proinflammatory T_H17 differentiation and neuroinflammation.

Funding

This study is supported by Fondation Leducq, France (Sphingosine 1-Phosphate in Neurovascular Biology and Disease [SphingoNet]).

Conflicts of interest

The authors have declared that no conflict of interest exists.

Acknowledgements

We thank Dr. Xiangyue Zhang and Lewis Yu for helping macrophage and APC-T cell co-culture experiments; Anna Tomczak for her suggestion to this manuscript. H.-C.T. and M.H.H. formulated the hypothesis, designed research and wrote this manuscript. H.-C.T. performed all experiments and data analysis in this research. K.N. and E.E. contributed to experiments related to macrophage and APC-T cell co-culture. E.H. performed histological analysis of the brain of LysM OE mice. T.H. contributed to experiments related to myeloid $S1P_1$ signaling.

Appendix A. Supplementary data

Supplementary data to this article can be found online at https://doi.org/10.1016/j.jaut.2019.06.001.

References

[1] S.A. Levesque, A. Pare, B. Mailhot, V. Bellver-Landete, H. Kebir, M.A. Lecuyer, et al., Myeloid cell transmigration across the CNS vasculature triggers IL-1beta-driven neuroinflammation during autoimmune encephalomyelitis in mice, J. Exp. Med. 213 (2016) 929–949.

[2] B. Ajami, J.L. Bennett, C. Krieger, K.M. McNagny, F.M. Rossi, Infiltrating monocytes trigger EAE progression, but do not contribute to the resident microglia pool, Nat. Neurosci. 14 (2011) 1142–1149.

[3] J.M. Rumble, A.K. Huber, G. Krishnamoorthy, A. Srinivasan, D.A. Giles, X. Zhang, et al., Neutrophil-related factors as biomarkers in EAE and MS, J. Exp. Med. 212 (2015) 23–35.

[4] M.K. Mishra, V.W. Yong, Myeloid cells - targets of medication in multiple sclerosis, Nat. Rev. Neurol. 12 (2016) 539–551.

[5] J.W. Prineas, E.E. Kwon, E.S. Cho, L.R. Sharer, M.H. Barnett, E.L. Oleszak, et al., Immunopathology of secondary-progressive multiple sclerosis, Ann. Neurol. 50 (2001) 646–657.

[6] V. Brinkmann, A. Billich, T. Baumruker, P. Heining, R. Schmouder, G. Francis, et al., Fingolimod (FTY720): discovery and development of an oral drug to treat multiple sclerosis, Nat. Rev. Drug Discov. 9 (2010) 883–897.

[7] T. Baumruker, A. Billich, V. Brinkmann, FTY720, an immunomodulatory sphingolipid mimetic: translation of a novel mechanism into clinical benefit in multiple sclerosis, Expert Opin. Investig. Drugs 16 (2007) 283–289.

[8] L. Kappos, E.W. Radue, P. O'Connor, C. Polman, R. Hohlfeld, P. Calabresi, et al., A placebo-controlled trial of oral fingolimod in relapsing multiple sclerosis, N. Engl. J. Med. 362 (2010) 387–401.

[9] J.A. Cohen, F. Barkhof, G. Comi, H.P. Hartung, B.O. Khatri, X. Montalban, et al., Oral fingolimod or intramuscular interferon for relapsing multiple sclerosis, N. Engl. J. Med. 362 (2010) 402–415.

[10] V. Devonshire, E. Havrdova, E.W. Radue, P. O'Connor, L. Zhang-Auberson, C. Agoropoulou, et al., Relapse and disability outcomes in patients with multiple sclerosis treated with fingolimod: subgroup analyses of the double-blind, randomised, placebo-controlled FREEDOMS study, Lancet Neurol. 11 (2012) 420–428.

[11] L. Kappos, A. Bar-Or, B.A.C. Cree, R.J. Fox, G. Giovannoni, R. Gold, et al., Siponimod versus placebo in secondary progressive multiple sclerosis (EXPAND): a double-blind, randomised, phase 3 study, Lancet 391 (2018) 1263–1273.

[12] M.L. Oo, S.H. Chang, S. Thangada, M.T. Wu, K. Rezaul, V. Blaho, et al., Engagement of S1P(1)-degradative mechanisms leads to vascular leak in mice, J. Clin. Investig. 121 (2011) 2290–2300.

[13] S. Thangada, K.M. Khanna, V.A. Blaho, M.L. Oo, D.S. Im, C. Guo, et al., Cell-surface residence of sphingosine 1-phosphate receptor 1 on lymphocytes determines lymphocyte egress kinetics, J. Exp. Med. 207 (2010) 1475–1483.

[14] H.C. Tsai, Y. Huang, C.S. Garris, M.A. Moreno, C.W. Griffin, M.H. Han, Effects of sphingosine-1-phosphate receptor 1 phosphorylation in response to FTY720 during neuroinflammation, JCI insight 1 (2016) e86462.

[15] C.S. Garris, L. Wu, S. Acharya, A. Arac, V.A. Blaho, Y. Huang, et al., Defective sphingosine 1-phosphate receptor 1 (S1P1) phosphorylation exacerbates TH17-mediated autoimmune neuroinflammation, Nat. Immunol. 14 (2013) 1166–1172.

[16] M.L. Allende, T. Yamashita, R.L. Proia, G-protein-coupled receptor S1P1 acts within endothelial cells to regulate vascular maturation, Blood 102 (2003) 3665–3667.

[17] B. Jung, H. Obinata, S. Galvani, K. Mendelson, B.S. Ding, A. Skoura, et al., Flow-regulated endothelial S1P receptor-1 signaling sustains vascular development, Dev. Cell 23 (2012) 600–610.

[18] M.H. Han, S.I. Hwang, D.B. Roy, D.H. Lundgren, J.V. Price, S.S. Ousman, et al., Proteomic analysis of active multiple sclerosis lesions reveals therapeutic targets, Nature 451 (2008) 1076–1081.

[19] I.M. Stromnes, L.M. Cerretti, D. Liggitt, R.A. Harris, J.M. Goverman, Differential regulation of central nervous system autoimmunity by T(H)1 and T(H)17 cells, Nat. Med. 14 (2008) 337–342.

[20] A. Arac, S.E. Brownell, J.B. Rothbard, C. Chen, R.M. Ko, M.P. Pereira, et al., Systemic augmentation of alphaB-crystallin provides therapeutic benefit twelve hours post-stroke onset via immune modulation, Proc. Natl. Acad. Sci. U.S.A. 108 (2011) 13287–13292.

[21] E. Bettelli, M. Pagany, H.L. Weiner, C. Linington, R.A. Sobel, V.K. Kuchroo, Myelin oligodendrocyte glycoprotein-specific T cell receptor transgenic mice develop spontaneous autoimmune optic neuritis, J. Exp. Med. 197 (2003) 1073–1081.

[22] C.H. Wu, T.C. Huang, B.F. Lin, Folate deficiency affects dendritic cell function and subsequent T helper cell differentiation, J. Nutr. Biochem. 41 (2017) 65–72.

[23] H. Lee, J. Deng, M. Kujawski, C. Yang, Y. Liu, A. Herrmann, et al., STAT3-induced S1PR1 expression is crucial for persistent STAT3 activation in tumors, Nat. Med. 16 (2010) 1421–1428.

[24] J. Liang, M. Nagahashi, E.Y. Kim, K.B. Harikumar, A. Yamada, W.C. Huang, et al., Sphingosine-1-phosphate links persistent STAT3 activation, chronic intestinal inflammation, and development of colitis-associated cancer, Cancer Cell 23 (2013) 107–120.

[25] Y. Liu, J. Deng, L. Wang, H. Lee, B. Armstrong, A. Scuto, et al., S1PR1 is an effective target to block STAT3 signaling in activated B cell-like diffuse large B-cell lymphoma, Blood 120 (2012) 1458–1465.

[26] G. Liu, K. Yang, S. Burns, S. Shrestha, H. Chi, The S1P(1)-mTOR axis directs the reciprocal differentiation of T(H)1 and T(reg) cells, Nat. Immunol. 11 (2010) 1047–1056.

[27] J.J. Liao, M.C. Huang, E.J. Goetzl, Cutting edge: alternative signaling of Th17 cell development by sphingosine 1-phosphate, J. Immunol. 178 (2007) 5425–5428.

[28] A. Eken, R. Duhen, A.K. Singh, M. Fry, J.H. Buckner, M. Kita, et al., S1P1 deletion differentially affects TH17 and Regulatory T cells, Sci. Rep. 7 (2017) 12905.

[29] B. Ajami, N. Samusik, P. Wieghofer, P.P. Ho, A. Crotti, Z. Bjornson, et al., Single-cell mass cytometry reveals distinct populations of brain myeloid cells in mouse neuroinflammation and neurodegeneration models, Nat. Neurosci. 21 (2018) 541–551.

[30] J.E. Hughes, S. Srinivasan, K.R. Lynch, R.L. Proia, P. Ferdek, C.C. Hedrick, Sphingosine-1-phosphate induces an antiinflammatory phenotype in macrophages, Circ. Res. 102 (2008) 950–958.

[31] H.C. Tsai, M.H. Han, Sphingosine-1-Phosphate (S1P) and S1P signaling pathway: therapeutic targets in autoimmunity and inflammation, Drugs 76 (2016) 1067–1079.

[32] Y. Gao, J.I. Basile, C. Classon, D. Gavier-Widen, A. Yoshimura, B. Carow, et al., STAT3 expression by myeloid cells is detrimental for the T- cell-mediated control of infection with Mycobacterium tuberculosis, PLoS Pathog. 14 (2018) e1006809.

[33] O. Arlt, A. Schwiebs, L. Japtok, K. Ruger, E. Katzy, B. Kleuser, et al., Sphingosine-1-phosphate modulates dendritic cell function: focus on non-migratory effects in vitro and in vivo, Cell. Physiol. Biochem. : international journal of experimental cellular physiology, biochemistry, and pharmacology 34 (2014) 27–44.

[34] K. Thomas, T. Sehr, U. Proschmann, F.A. Rodriguez-Leal, R. Haase, T. Ziemssen, Fingolimod additionally acts as immunomodulator focused on the innate immune system beyond its prominent effects on lymphocyte recirculation, J. Neuroinflammation 14 (2017) 41.

[35] A. Finley, Z. Chen, E. Esposito, S. Cuzzocrea, R. Sabbadini, D. Salvemini, Sphingosine 1-phosphate mediates hyperalgesia via a neutrophil-dependent mechanism, PLoS One 8 (2013) e55255.

[36] V.A. Blaho, T. Hla, An update on the biology of sphingosine 1-phosphate receptors, J. Lipid Res. 55 (2014) 1596–1608.

[37] M. Prinz, D. Erny, N. Hagemeyer, Ontogeny and homeostasis of CNS myeloid cells, Nat. Immunol. 18 (2017) 385–392.

[38] D. Mrdjen, A. Pavlovic, F.J. Hartmann, B. Schreiner, S.G. Utz, B.P. Leung, et al., High-dimensional single-cell mapping of central nervous system immune cells reveals distinct myeloid subsets in Health, aging, and disease, Immunity 48 (2018) 599.

[39] Q. Li, Z. Cheng, L. Zhou, S. Darmanis, N.F. Neff, J. Okamoto, et al., Developmental heterogeneity of microglia and brain myeloid cells revealed by deep single-cell RNA sequencing, Neuron 101 (2019) 207–23 e10.

[40] J.A. Cohen, A. Bar-Or, B.A.C. Cree, Y. Mao-Draayer, M.H. Han, B. Singer, et al., The FLUENT study design: investigating immune cell subset and neurofilament changes in patients with relapsing multiple sclerosis treated with fingolimod, Multiple sclerosis journal - experimental, translational and clinical 5 (2019) 2055217318819245.